ORIENTAL JOURNAL OF CHEMISTRY
An International Open Access, Peer Reviewed Research Journal
www.orientjchem.org
ISSN: 0970-020 X
CODEN: OJCHEG
2025, Vol. 41, No.(2):
Pg. 393-398

Synthesis and Characterization of Excess and Deficit of Iron in $LaFeO_3$[$LaFe_{1.05}O_3$ and $LaFe_{0.95}O_3$] inorganic perovskite materials using simple and efficient Sol-gel technique with Magnetic Properties

K. RAMMOHAN[1*,3], G. VIJAYA LAKSHMI[1*,2] and G. RAMESH[4]

[1]Department of Chemistry, University College of Science, Osmania University, Hyderabad, Telangana-500007, India.
[2]Department of Chemistry, Veeranari Chakali Ilamma Women's University, Koti, Hyderabad, Telangana-500095, India.
[3]Department of M.Sc. 5 Year Integrated Chemistry, University P.G. College, Palamuru University, Mahbubnagar, Telangana-509001, India.
[4]Department of Chemistry, Vardhaman College of Engineering, Hyderabad-501218,Telangana, India.
*Corresponding author E-mail: patriji2095@gmail.com

http://dx.doi.org/10.13005/ojc/410207

(Received: February 01, 2025; Accepted: March 28, 2025)

ABSTRACT

The sol-gel method was used to create $LaFeO_3$(LFO) perovskites with abundant iron and deficit iron ($LaFe_{1.05}O_3$ and $LaFe_{0.95}O_3$). Vibrating sample magnetometry (VSM) analysis, X-ray Photoelectron Spectroscopy (XPS), UV-Visible Diffuse Reflectance Spectrometry, Powder X-ray Diffraction and Field Emission Scanning Electron Microscopy and Energy Dispersive Spectroscopy were used to thoroughly describe the materials.The orthorhombic-shaped iron-modified LFO perovskites that crystallised in the Pnma space group were successfully synthesised, as proven by the p-XRD. The FESEM investigation revealed uneven morphology and phase purity. EDS and XPS examination of the following perovskites elemental composition, surface structure, and valence state of the chemical. UV-Vis DRS was used to determine the energy band gap of $LaFe_{1.05}O_3$ (1.98eV) and $LaFe_{0.95}O_3$ (2.03eV). Iron-deficient $LaFeO_3$ ($LaFe_{0.95}O_3$) showed paramagnetic behaviour with increased saturation magnetisation (MS), while $LaFe_{1.05}O_3$ (with abundant iron) shows weak ferromagnetic behaviour according to VSM research.

Keywords: Perovskites, Iron excess, Iron deficiency, VSM analysis, Magnetic characteristics and Paramagnetism.

INTRODUCTION

With the chemical formula ABO_3, perovskite is a mineral that can be yellow, brown, or black. Perovskite was at first found by German geologist Gustav Rose in 1839 in the Ural Mountains[1], it was named after Russian mineralogist Lev A. Perovski. Lev A. Perovski found a crystal structure that is

cubic using the chemical $CaTiO_3$ framework. Ions form an octahedron around cation B in perovskite crystals, and cation A is in the middle of the BO6 octahedron, joined at the angle of the apex. Anions can coordinate in six dimensions[2,3]. Because they can do many things, their chemical and physical properties are very interesting. Some of these are ferroelectricity, half-metallicity, a high dielectric constant, excitation-binding energy, long-range ambipolar charge transport, a high absorption coefficient, and optoelectricity[4-6].

The perovskite narrative really heats up in the twenty-first century. Interest in the structure has significantly increased in recent years. Perovskites are widely used in magnetic devices and solid oxide fuel cells, electrical conductors, as well as catalysis. Perovskites are materials that are very stable at high temperatures and in chemicals. They are also paramagnetic, photocatalytic, thermoelectric, and dielectric, and they can conduct electricity. High sensitivity to oxygen and compounds containing oxygen is ensured by iron at the B-site, the perovskite structure's "catalytic" location[7–10].

Both too much and too little iron using powder XRD, X-Ray Photoelectron Spectroscopy, FESEM-EDS, UV-Visible Diffuse Reflectance spectrometry, VSM. $LaFeO_3$ perovskites were created using the sol-gel method. This study's results suggest that the sol-gel method could be used to make fine above perovskites with a 98% yield. The above perovskites having an orthorhombic configuration that crystallised inside the orthorhombic Pnma space group were successfully synthesised, according to the results[11,12]. La^{+3} has eight coordinates and is joined to eight O_2 atoms. The current work aims to prepare iron-based perovskites and is an attempt in that direction. Higher saturation magnetisation (MS) and paramagnetic behaviour were demonstrated by these synthesised perovskites, which also absorbed more visible light during photodegradation. Therefore, in the process of photodegradation, these perovskites function as a photocatalyst.

The impact of stoichiometry for iron on the structural and magnetic characteristics of perovskites with LFO which are produced by an effective sol-gel process is clarified by this work.

MATERIALS AND METHODS

Hexahydrate of lanthanum(III) nitrate ($La(NO_3)_3.6H_2O$) were supplied by Research Labs of Sisco Pvt. Ltd. in Taloja, Maharashtra, India. We obtained nitrate nonahydrate of iron(III) ($Fe(NO_3)_3.9H_2O$) from Virat Lab in Mumbai, India. The fine chemistry research facility in Mumbai, India, provided the ethyl alcohol (C_2H_5HO), ethylene glycol (EG, HO-C_4H_4OH), citric acid (HOC(CO_2H)($CH_2CO_2H)_2$), and ammonia (NH_3). No additional eradication was required, as the solvents utilized in this process are analytical reagent-grade.

Synthesis of pure iron excess and deficit in $LaFeO_3$ perovskites by the sol-gel method

Sol-gel synthesis of iron excess and deficit in LFO perovskites

The perovskite LFO powders were created using calcination and sol-gel techniques. Five grammes of $La(NO_3)_3.6H_2O$ and 4.8 g of $Fe(NO_3)_3.9H_2O$ (in a ratio of 1:1.05), as well as 5 g of $La(NO_3)_3.6H_2O$ and 4.4 g of $Fe(NO_3)_3.9H_2O$ (in a ratio of 1:0.95), were the starting materials. They were dissolved in 200 millilitres of ethyl alcohol in a 500 millilitre beaker and left to stir at room temperature for two hours. 5.05 g citric acid solution was introduced to the mixture. After 5.5 g of citric acid had been stirred for two hours. A soluion of ammonia was introduced to adjust the pH scale down to 7 at 70°C after an hour of stirring. 3.2 millilitres of the solution of ethylene glycol was added to 100 millilitres of a 50% solution at 160°C after 3.6 millilitres of ethylene glycol had been stirred for an hour. Before being grounds for calcinations in a muffle furnace at 800°C for eight hours, the mixture was agitated until it turned black. As a result, the powdered LFO perovskite materials had a 98% absolute excess and deficit of iron.

The following reaction occurs in the creation of excess iron in $LaFe_{1.05}O_3$ perovskite material:

$$1La(NO_3)_3.6H_2O + 1.05\,Fe(NO_3)_3.9H_2O + C_6H_8O_7.H_2O \longrightarrow LaFe_{1.05}O_3 + 6CO_2 + 3N_2 + nH_2O$$

The following reaction occurs in the creation of deficit iron in $LaFe_{1.05}O_3$ perovskite material:

$$1La(NO_3)_3.6H_2O + 0.95\,Fe(NO_3)_3.9H_2O + C_6H_8O_7.H_2O \longrightarrow LaFe_{0.95}O_3 + 6CO_2 + 3N_2 + nH_2O$$

RESULTS AND DISCUSSIONS

UV-Visible spectroscopy

Figure 1 displays the iron surplus and deficiency UV-Vis DRS spectra in LFO produced using the sol-gel technique. 617 nm and 603 nm[13] were determined to be the maximum wavelengths. The closer the species are to one another, the greater the absorption. This suggests a closer relationship

between the species involved in the iron deficiency and excess in the LFO structures formed through the sol-gel process. In the visible wavelength region of[14], maximum value indicates that LFO produced using this technique is active as a photocatalyst.

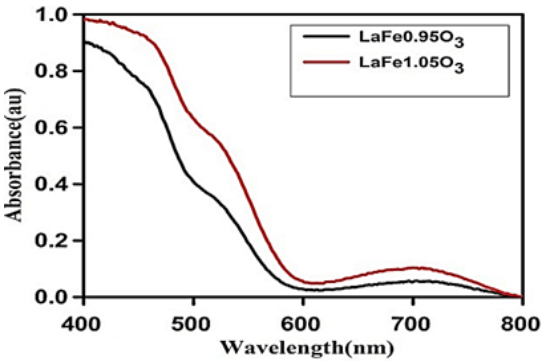

Fig. 1. UV-Visible Diffuse Reflectance Spectrometry powdered samples of Sol-Gel synthesised perovskites

Band gap energy

Plots of Kubelka-Munk (KM) of synthesised perovskites[15] are displayed in Fig. 2. The bandgaps of LFO nanoparticles with excess and deficient iron are 1.98eV and 2.03eV, accordingly. These values are helpful for more photocatalysis research because they are less than the orthorhombic LFO perovskites bandgap energies.

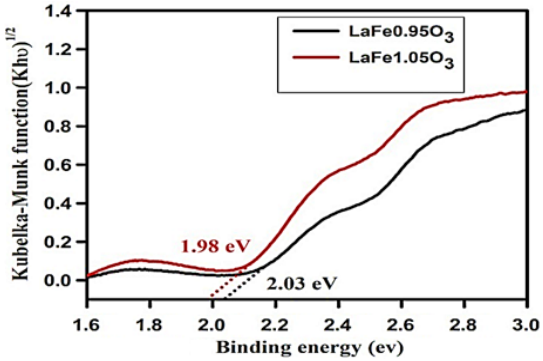

Fig. 2. Band gap energy of synthesised perovskites plotted by KM

XRD

By contrasting the outcomes with the typical JCPDS card numbers 88-0641, respectively[16], diffraction of X-ray examination verified the powder was made up of synthesised compounds that have an orthorhombic configuration that crystallized in the group of an orthorhombic Pnma space. Crucially, the perovskite structure was the only secondary phase detected. Using the formula $d = (h^2/a^2+k^2/b^2+l^2/c^2)^{-1/2}$ where (d) is the interplanar distance, a,b,c and h,k,l are lattice variables and indices of crystallographic planes[17], compound's lattice parameters were found using X-Ray Diffraction Pattern. The sol-gel approach yielded powdered synthesised perovskites with a = 5.5647A°, b = 7.8551A°, c = 5.556A° values. The unit cell volumes of the synthesised chemicals are 242.86 A°3. Synthesised perovskites exhibit orthorhombic structure in their X-ray diffraction (XRD) patterns (Figure 3).

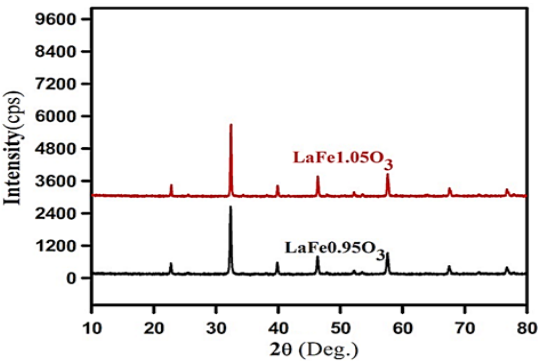

Fig. 3. The diffraction pattern of X-ray powdered synthesised perovskites

FESEM and EDS

Iron overload and deficiency in LFO perovskite18 were investigated using FESEM and EDS spectra. Large, irregularly shaped lumps that adhere to one another are shown in FESEM pictures of excess LFO perovskite and iron deficiency. The EDS analysis confirms the accurate amounts of La, Fe, and O chemicals in pure $LaFeO_0$ perovskites. Each element's weight proportion is shown in the relevant EDS statistics. Fig. 4 and 5 show that the FESEM and EDS results for iron-containing LFO perovskites excess and deficit don't change much.

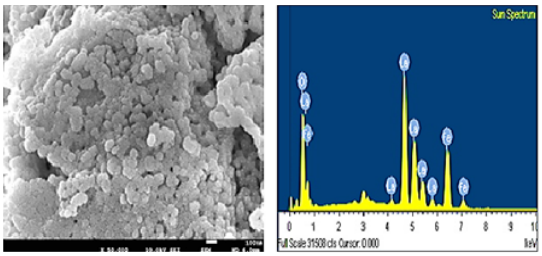

Fig. 4. FESEM-EDS of LFO's iron deficiency

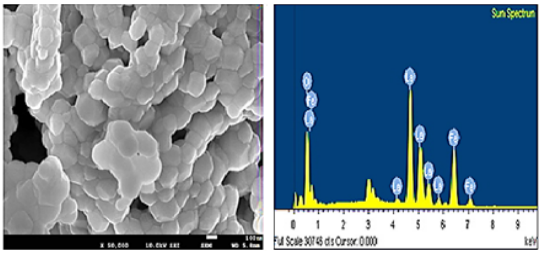

Fig. 5. FESEM-EDS of LFO's iron excess

XPS

Data on the binding energies of synthetic materials are shown in panels a–d of Fig. 6 and 7. The iron excess and deficit of the LFO-800 nanostructure XPS survey spectrum are shown in Fig. 6a and 7a. The coexistence of lanthanum (La), oxygen (O), and iron (Fe) in the sample is approved, and distinct elemental peaks are not identified. The basic spectra of La^{3+} In the oxide shape were assigned to the two significant signals that La displayed simultaneously at 836.94eV, 865.73eV (Fig. 6b and 7b)[19]. Based on the high- firmness of XPS analysis in iron (Figs. 6c,7c) which displayed distinct peaks with two binding energies of Fe $2p_{3/2}$ and Fe $2p_{1/2}$ at 710.86eV, 724.70eV, and 743.65eV (standard values: $Fe2p_{1/2}$-852.6eV; $Fe2p_{3/2}$-869.3eV), Fe is present in Fe^{3+} oxidation states in the LaF_eO_3-800[20]. The fitted binding energies also showed lower and higher binding energies after La-Fe interactions. Located at 530.30eV, 532.10eV two peaks in Fig. 6d and 7d indicated the presence of oxygen (O^{2-}) in the $LaFeO_3$ perovskite lattice. Utilising the aforementioned helpful information from the XPS survey is recommended. That is very similar to the excess of LFO and the chemical structure of iron deficiency.

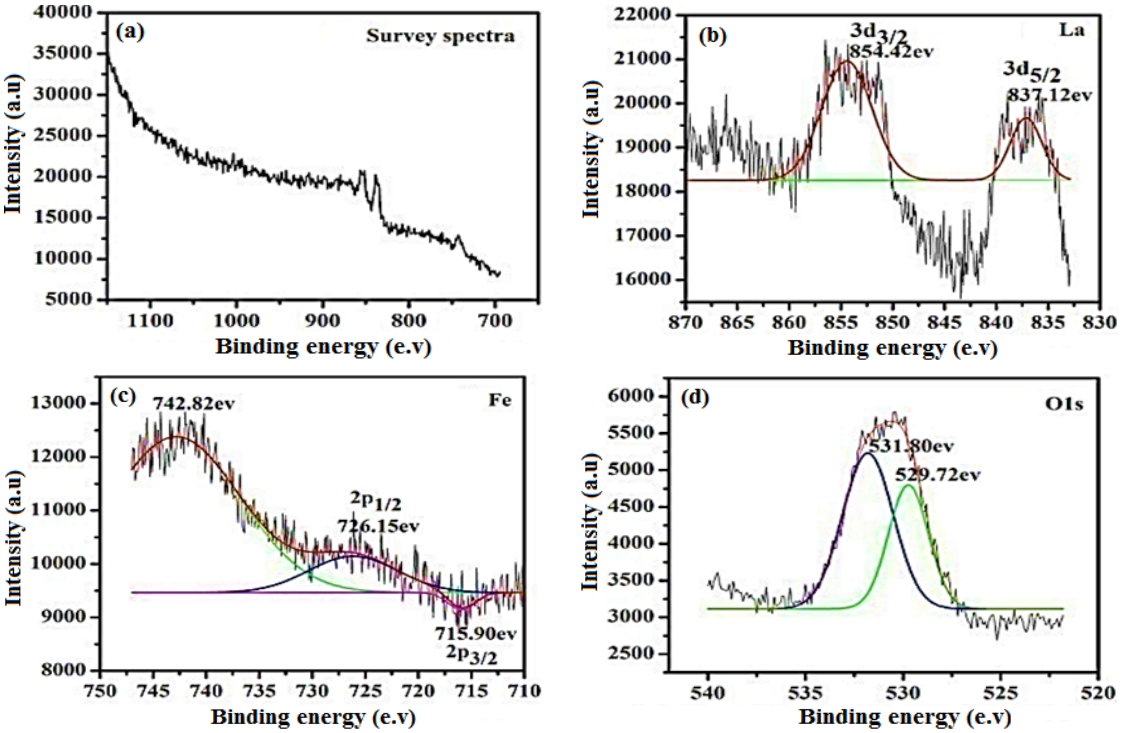

Fig. 6. LFO-800 XPS spectra photocatalyst's iron deficiency: Survey spectra (a) La3d (b)Fe 2p (c), O 1s (d)

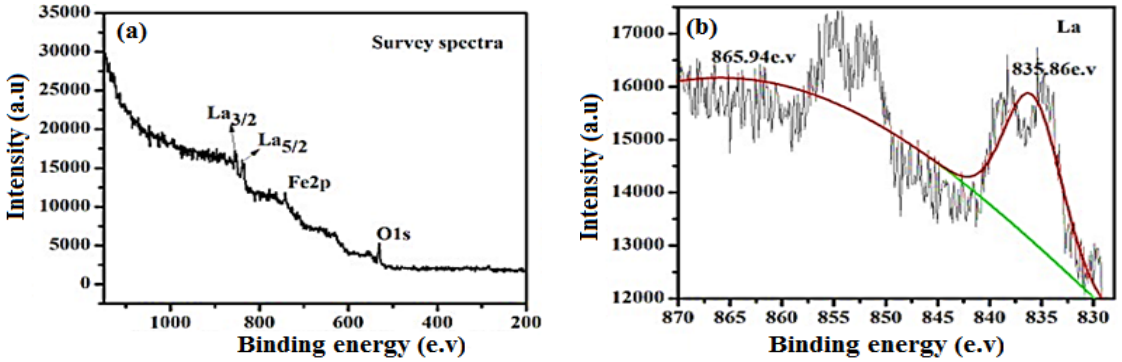

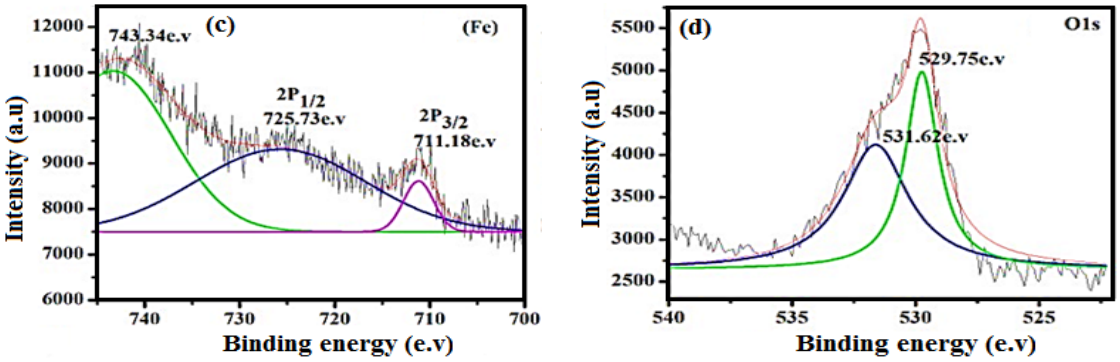

Fig. 7. LFO-800 XPS spectra photocatalyst's iron excess: Survey spectra (a), La3d (b), Fe 2p (c), and O1s (d)

VSM analysis

The magnetisation Field (H) and (M) hysteresis loops seen in Fig. 9 were recorded at 250C using a vibrating sample magnetometer (VSM). As stated by Gehring[21,22] and The statistical distribution of Fe^{3+} in the octahedron structure may be the origin of bulk magnetisation and mild ferromagnetism, and the development of lattice defects may also lead to these phenomena. Fig. 8 in this paper displays the room temperature magnetisation for synthesised perovskites at different magnetic fields of 20 kOe. $LaFe_{0.95}O_3$ (with iron deficit) shows paramagnetic behaviour and higher saturation magnetisation (M) among the two samples under study, while $LaFe_{1.05}O_3$ (with abundant iron) shows weak ferromagnetic behaviour, as reported. $LaFe_{0.95}O_3$ perovskites function as efficient photocatalysts by, while is occurring, absorbing more visible light.

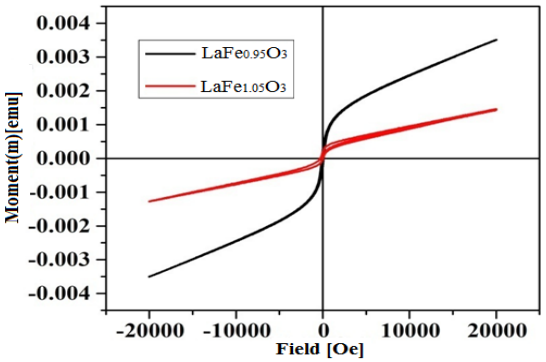

Fig. 8. VSM investigation of iron abundance and deficit in $LaFeO_3$ perovskite materials

CONCLUSION

This study shows how the amount of iron in an LFO perovskites mixture changes its structure and magnetic properties when it is made using a good sol-gel method. An FESEM and p-XRD analysis showed that the compounds in question had an irregular shape, an orthorhombic structure, and a pure phase. Using EDS and XPS analysis, Elemental composition tracked down surface structure, valence state of chemical the important components of the aforementioned perovskites. Iron-deficient $LaFexO_3$ ($LaFe_{0.9}5O_3$) showed paramagnetic behaviour with increased saturation magnetisation (MS), while $LaFe_{1.05}O_3$ (with abundant iron) shows weak ferromagnetic behaviour according to VSM research.

These results should be expanded by more research on how iron stoichiometry affects other functional characteristics like electrical conductivity or catalytic activity.

ACKNOWLEDGMENT

For providing the required infrastructure, the authors would like to thank CFRD-OU and the Department of Chemistry at Osmania University.

Conflict of interest

Any financial, personal, or other links with other individuals or organisations that may have an impact on their work are among the conflicts of interest that all writers are asked to declare.

REFERENCES

1. Shi, D.; Adinolfi, V.; Comin, R.; Yuan, M.; Alarousu, E.; Buin, A.; Chen, Y.; Hoogland, S.; Rothenberger, A.; Katsiev, K.; Losovyj, Y.; Zhang, X.; Dowben, P. A.; Mohammed, O. F.; Sargent, E. H.; Bakr and O. M., *Science.*, **2015**, *347*, 519-522.
2. Yang, W. S.; Park, B. W.; Jung, E. H.; Jeon, N. J.; Kim, Y. C.; Lee, D. U.; Shin, S. S.; Seo, J.; Kim, E. K.; Noh, J. H.; Seok and S. I., *Science.,* **2017**, *356*, 1376-1379.

3. Heo, S.; Seo, G.; Lee, Y.; Lee, D.; Seol, M.; Lee, J.; Park, J. B.; Kim, K.; Yun, D. J.; Kim, Y. S.; Shin, J. K.; Ahn, T. K.; Nazeeruddin and M. K., *Energy Environ. Sci.*, **2017**, *10*, 1128-1133.
4. Saliba, M.; Matsui, T.; Domanski, K.; Seo, J.-Y.; Ummadisingu, A.; Zakeeruddin, S. M.; Correa-Baena, J.-P.; Tress, W. R.; Abate, A.; Hagfeldt, A and Gratzel, M., *Science.*, **2016**, *354*, 206-209.
5. Alharbi, E. A.; Alyamani, A. Y.; Kubicki, D. J.; Uhl, A. R.; Walder, B. J.; Alanazi, A. Q.; Luo, J.; Burgos-Caminal, A.; Albadri, A.; Albrithen, H.; Alotaibi, M. H.; Moser, J. E.; Zakeeruddin, S. M.; Giordano, F.; Emsley, L and Gratzel, M., *Nat. Commun.*, **2019**, *10*, 3008.
6. Ahn, N.; Son, D. Y.; Jang, I. H.; Kang, S. M.; Choi, M.; Park and N. G., *J. Am. Chem. Soc.*, **2015**, *137*, 8696-8699.
7. Huang, P.; Chen, Q.; Zhang, K.; Yuan, L.; Zhou, Y.; Song, B. and Li. Y., *J. Mater. Chem.*, A., **2019**, *7*, 6213-6219.
8. Park, B. W.; Philippe, B.; Jain, S. M.; Zhang, X.; Edvinsson, T.; Rensmo, H.; Zietz, B.; Boschloo, G. J., *Mater. Chem.*, **2015**, *3*, 21760-21771.
9. Liu, X.; Wang, Y.; Xie, F.; Yang, X.; Han, L., *ACS Energy Lett.*, **2018**, *3*, 1116-1121.
10. Guerrero, A.; You, J.; Aranda, C.; Kang, Y. S.; Garcia-Belmonte, G.; Zhou, H.; Bisquert, J.; Yang, Y., *ACS Nano.*, **2016**, *10*, 218-224.
11. Shi, D.; Adinolfi, V.; Comin, R.; Yuan, M.; Alarousu, E.; Buin, A.;Chen, Y.; Hoogland, S.; Rothenberger, A.; Katsiev, K.; Losovyj, Y.;Zhang, X.; Dowben, P. A.; Mohammed, O. F.; Sargent, E. H.; Bakr, O.M., *Science.*, **2015**, *347*, 519-522.
12. Aristidou, N.; Eames, C.; Sanchez-Molina, I.; Bu, X.; Kosco, J.; Islam, M. S.; Haque, S. A., *Nat. Commun.*, **2017**, *8*, 15218.
13. Yang, W. S.; Park, B.-W.; Jung, E. H.; Jeon, N. J.; Kim, Y. C.; Lee, D. U.; Shin, S. S.; Seo, J.; Kim, E. K.; Noh, J. H., *Science.*, **2017**, *356*, 1376-1379.
14. Prasanna, R.; Gold-Parker, A.; Leijtens, T.; Conings, B.; Babayigit, A.; Boyen, H. G.; Toney, M. F.; McGehee, M. D., *J. Am. Chem. Soc.*, **2017**, *139*, 11117- 11124.
15. Mekhemer, Gamal AH., *Scientific Reports.*, **2023**, *13*(1), 7453.
16. Hammouda.; Samia Ben., *Applied Catalysis B: Environmenta.*, **2018**, *233*, 99-111.
17. Koj$_0$inovi.; Jelena., *Materials Chemistry Frontiers.*, **2022**, *6*(9), 1116-1128.
18. Wu.; Mudi., *Science of The Total Environment.*, **2021**, *795*, 148904.
19. Abdel-Khalek, E. K., *Physica B: Condensed Matter.*, **2022**, *624*, 413415.
20. Kim.; Bae-Jung., *Journal of the American Chemical Society.*, **2019**, *141*(13), 5231-5240.
21. Chang.; Hui., *ACS catalysis.*, **2020**, *10*(6), 3707-3719.
22. Nenning.; Andreas., *The Journal of Physical Chemistry C.*, **2016**, *120*(3), 1461-1471.